Astron. Astrophys. 335, 1040–1048 (1998)

ASTRONOMY AND ASTROPHYSICS

Discovery of multiple non-axially symmetric near-IR bow shocks around the pre-main sequence binary AFGL 961

Colin Aspin

Nordic Optical Telescope, Apartado 474, E-38700 Santa Cruz de la Palma, Islas Canarias, Spain

Received 12 February 1998 / Accepted 14 April 1998

Abstract. We present the discovery of multiple non-axially symmetric near-IR molecular hydrogen bow shocks around the high-mass pre-main sequence binary system AFGL 961. These data indicate that at periods one or both components of the binary have produced collimated outflows with associated shocks similar to those observed at visual wavelengths resulting in optical Herbig-Haro objects. We detect a minimum of four nebulous structures reminiscent of optical bow shocks together with five other diffuse objects with less well-defined morphology. The spatial location of the bow shocks and associated nebulous knots suggests that both components of the binary have, at times, actively driven outflows. At the present time, only the western component of the binary currently shows direct evidence of outflow activity in the form of ^{12}CO emission bandheads. The timescale between the outbursts that drive the outflows and result in the creation of the NIR shock-excited nebulae is 300–500 years. This is similar to estimates made for related events in both optical Herbig-Haro sources and FU Orionis type stars.

Key words: circumstellar matter – stars: individual: AFGL 961 – stars: pre-main sequence – ISM: jets and outflows – infrared: ISM: lines and bands

1. Introduction

There now exist numerous examples of collimated outflows and jets from young, pre-main sequence (PMS) stars. Many such phenomena have been imaged in the optical where they manifest themselves via shock-excited nebulous structures generally referred to as Herbig-Haro (HH) objects (Herbig 1951; Böhm et al. 1973) and Herbig-Haro jets (e.g. HH 46/47, Dopita, Evans & Schwartz, 1982; HH 34, Reipurth & Heathcote, 1992; HH 111, Reipurth, 1989). Also often present in outflows with HH objects are parabolic bow shock structures indicating the existence of a 'working-surface' where the outflowing gas jet impacts on and interacts with either ambient molecular cloud material or earlier ejecta from the young star. A excellent example of an optical bow shock is found in the source HH 34 (Reipurth & Heathcote, 1992). In this object a large parabolic emission feature is located beyond, and along the axis of, a thin high-velocity HH jet originating close to the young star (cf. HST WFPC2 image in PRC95-24a). Some collimated outflows, however, cannot be studied in the optical since they remain deeply embedded in the dense molecular cores out of which the associated young stellar objects (YSOs) are forming. These objects are obscured by perhaps A_V $\sim$100 magnitudes of extinction. Some of these embedded sources have been imaged with highly sensitive, large-format near-IR (NIR) arrays instruments and it is becoming clearer that similar morphological structures as seen in the optical are present also in shock-excited NIR emission, specifically in the lines of molecular hydrogen (H_2). Good examples of such sources are HH 211 (McCaughrean, Rayner & Zinnecker 1994), L1634 (Hodapp & Ladd, 1995; Eislöffel, 1997) and L1448 (Davis et al., 1994a). In addition, many optically detected HH objects and jets have subsequently been studied in the NIR (e.g. HH 46/47, Eislöffel et al., 1994; HH 1/2, Davis et al., 1994b). In these objects shock-excited H_2 emission is often observed coincident with, or closeby, regions of optical shock-excited emission. Below, we presented the discovery of multiple NIR bow shocks structures and associated nebulosities around the PMS binary AFGL 961. Whether these objects are the NIR counterparts of optical shock-excited emission nebulae i.e. the NIR equivalent of optical HH objects, or are purely NIR emission nebulae is unclear due to overlying extinction. However, to date, such structures, especially associated with high-mass, high-luminosity PMS binaries, are unique and are suggestive of a high level of outflow activity in the source in the recent past.

The source AFGL 961 (Grasdalen, et al. 1983) is a well known and well studied high-mass, high-luminosity (L_{bol} $\sim$7500$L_\odot$, Castelaz, et al. 1985) binary PMS star system located in the outskirts of the Rosette Nebula (Lenzen, et al. 1984). The region surrounding AFGL 961 is optically obscured by the associated molecular cloud core, however, the two stellar components of the system are easily detected in the NIR. These two sources are both classified as early-B type PMS stars and are separated by $\sim$6″ or, at the distance of AFGL 961 (d$\sim$1.6kpc, Turner, 1976), 9600 A.U. or 0.04pc. Both stars possess 2.166μm Br-γ emission and an associated bipolar CO molecular outflow (Lada & Gautier 1982) enamates from their location and ex-

Send offprint requests to: C. Aspin

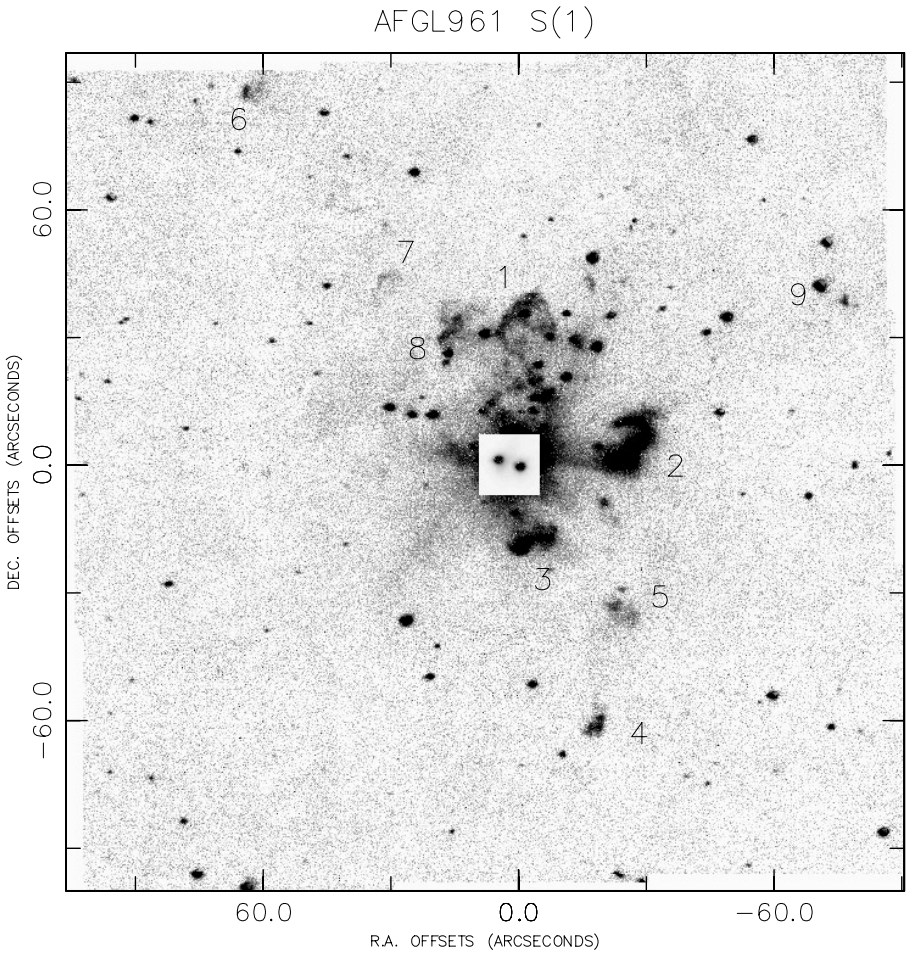

Fig. 1. A mosaic image of the AFGL 961 region using the narrow band 2.122μm v=1-0 S(1) H_2 filter covering $\sim 3.25' \times 3.25'$. The major H_2 nebulous objects are indicated and designated with AS numbers 1 through 9. To allow the two stellar sources to be seen, a low-contrast image of the region immediately surrounding these sources has been superimposed on the high-contrast mosaic.

tending preferentially to the north-east and south-west[1]. There exists an associated IRAS source, 06319+0415, centred on the binary with fluxes F_ν at 12 μm, 25 μm, 60 μm, 100 μm of 78 Jy, 375 Jy, 959 Jy and 995 Jy, respectively. NIR K-band images of the region presented by Hodapp (1994) show it to be morphologically complex with extensive nebulosity surrounding the central binary. Hodapp suggested that a small stellar PMS cluster may be present around AFGL 961 including the bright PMS star, designated AFGL 961 W, $\sim 30''$ to the west of the binary. Due to this previous designation, we herein refer to the eastern and western AFGL 961 binary components as AFGL 961a and AFGL 961b, respectively.

The two stars forming the AFGL 961 binary were included in a 2μm spectroscopic survey of young, high-mass, high-luminosity, pre-main sequence object we performed at the UKIRT telescope. During this survey we detected strong molecular hydrogen (H_2) emission to both the north and south of AFGL 961b. This discovery led us to a more focussed observing campaign. The results of this study are presented below. We show that AFGL 961 possess numerous shock-excited nebulous H_2 objects located along many different axes from the sources and lying up to $\sim 110''$ (0.85pc at 1.6kpc) distant. Several of these nebulous objects are similar in morphology to optical HH bow shocks. Below we discuss the discovery, nature and possible history of these multiple, non-axially symmetric H_2 bow shock structures.

[1] A recent higher spatial resolution CO map of the AFGL 961 outflow has been obtained and will be published in Sandell & Aspin (1998).

2. Observations

Imaging data on AFGL 961 using a narrow band (2%) molecular hydrogen (H_2) filter centred on the λ2.122μm v=1-0 S(1) line were acquired on UT Feb 9, 1996 at the United Kingdom Infrared Telescope, Mauna Kea, Hawaii using the facility 1–5μm camera, IRCAM3. This instrument, based on a 256×256 Santa Barbara Research Center (SBRC) InSb detector, is described in detail in Puxley et al. (1994). Using a pixel scale $0.286''$/pixel, we obtained a small mosaic of images (3x3) with an exposure time per tile of 5 minutes. The final mosaic image, shown in Fig. 1, covers a spatial area of $\sim 3.25'$ square. A low-contrast version of the central region is overlaid on the image to indicate the location of the AFGL 961 binary stars. A contour map of the central region of this mosaic image showing the area immediately surrounding the binary is presented in Fig. 2. The images were dark subtracted, flat-fielded using a median-filtered flat-field calculated from the object images, and mosaiced in the usual manner. We refer the reader to Aspin, Sandell & Russell (1994) for specific details of the data reduc-

Table 1. Positions and Descriptions of Nebulous Objects

CA No.	Offset wrt AFGL 961b ″E,″N	Position Angle (degrees) E of N	Description
1	-2,+39	354°	large bow shock
2	-28,+6	270–291°	cavity walls/shell structure
3	-1,-19	178°, 157°	two small bow shocks
4	-18,-61	164°	fainter small bow shock
5	-23,-33	214°	knots/diffuse nebula
6	+65,+88	36°	knots/diffuse nebula
7	+33,+44	36°	faint small bow shock
8	+22,+16	36–40°	knots/diffuse nebula, possible very faint bow shock
9	-71,+42	289°	knots/diffuse nebula, possible star

Offsets are in arcseconds and are +ve east and north.
'bow shock' indicates a strong resemblance to an optical HH bow shock.
'knot' indicates a relatively compact nebulous structure.
'diffuse' indicates an extended diffuse nebulous emission.

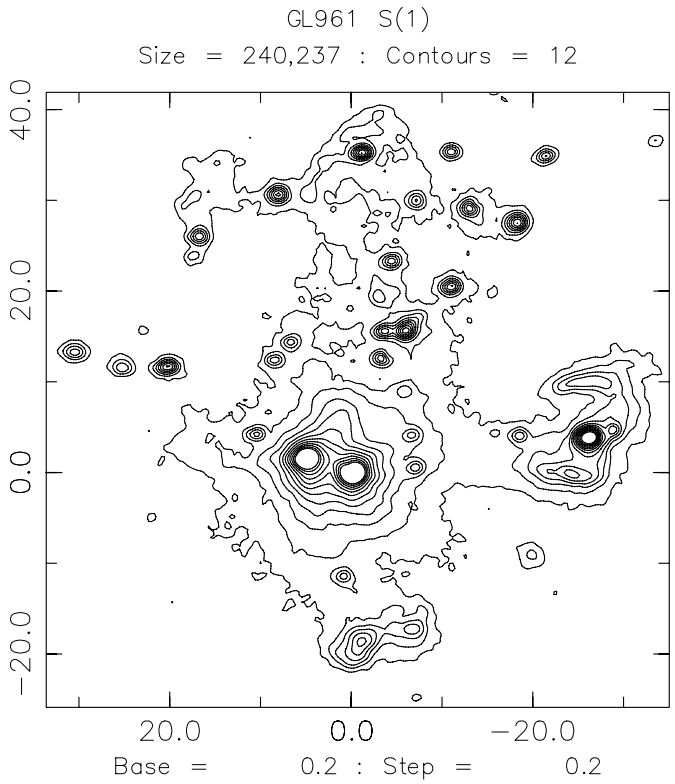

Fig. 2. Contour map of the central region of the mosaic S(1) image of AFGL 961. AFGL 961 W is the region from -20″ West to the western edge of the image. The image has been sky subtracted and the contours are in ADU/sec in steps of 2 ADU/sec from a base of 0.5 ADU/sec.

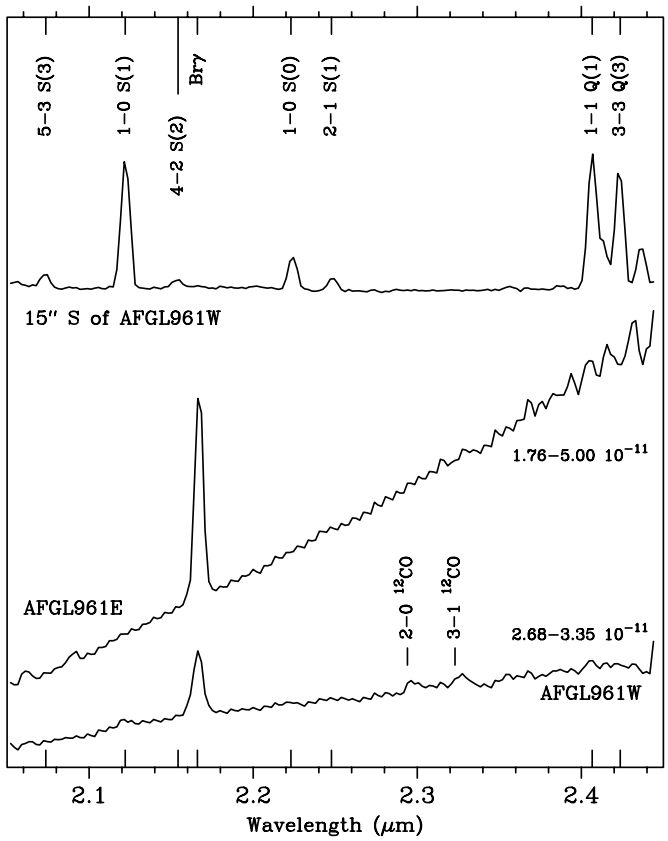

Fig. 3. 2μm spectroscopy of AFGL 961a and AFGL 961b. Also shown is the spectrum of nebulosity 15″ south of AFGL 961b. The range of numbers associated with the AFGL 961a and AFGL 961b spectra are the fluxes at the extremely of the spectra in Watts m^{-2} μm^{-1}.

tion techniques used. No observations of a standard star were obtained due to the presence of thin variable cirrus during the observations. Astronomical seeing during the observations was ∼0.75″.

Spectroscopy of AFGL 961a and AFGL 961b was obtained several years before the imaging data, specifically on UT Dec 28, 1993. These data were also acquired at the UKIRT and utilized the facility cooled-grating spectrometer, CGS4, also based on a 256×256 SBRC InSb array and which is described in detail in Mountain, et al. (1990). The CGS4 slit was positioned North-South and two spectra were acquired centred on AFGL 961a and AFGL 961b, respectively. The slit was ∼90″ in extent and

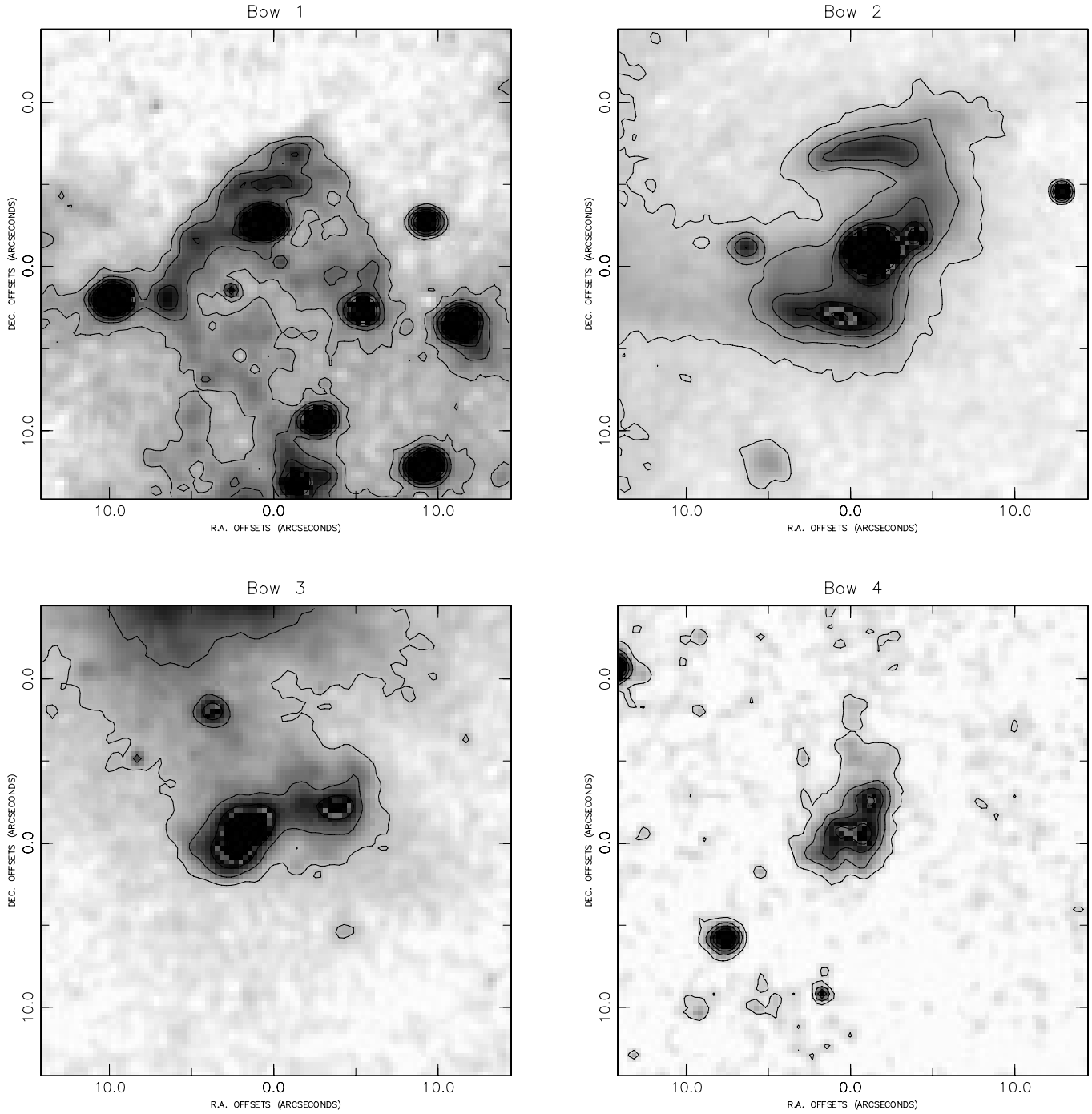

Fig. 4. S(1) contour plots superimposed on grey scale images of CA 1,2,3 and 4 extracted from the full AFGL 961 image. The contours shown are in ADU/sec. For CA 1 (top left) the contours base is 0.15 with a step of 0.1. For CA 2 (top right) and CA 3 (bottom left) the contour base is 0.15 with a step of 0.2. For CA 4 (bottom right) the contour base is 0.05 with a step of 0.1.

therefore we obtained simultaneous spectra of the two stellar source and of the regions $\pm 45''$ to both north and south of each. The spectra were acquired using the 75 l/mm grating resulting on a spectral resolution of $\sim$1000 over the wavelength range 2.05–2.45μm. The spectra were sky-subtracted after preliminary processing (bias subtraction, flat-fielding) using blank sky observations taken interspersed between multiple target observations. The target spectra were extracted from the spectroscopic images and ratioed with observations of a standard star taken at a similar airmass. This effectively removed atmospheric effects/bands. These standard star observations also allow us to flux-calibrate the target spectra. For these data, observations of the bright standard star BS2845 (B8Ve, K=3.04) were used. The Brγ present in the spectrum of this star was

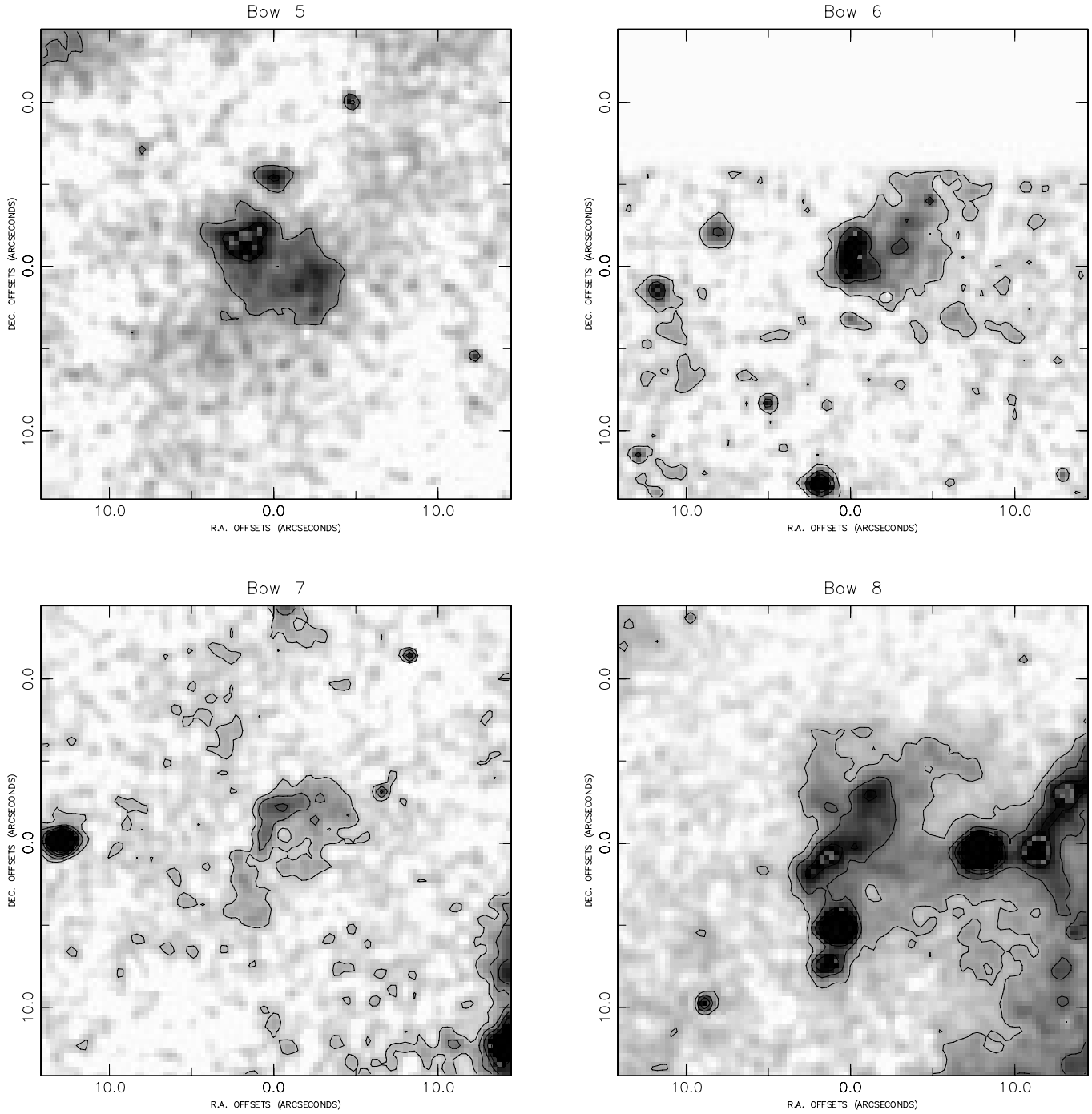

Fig. 5. S(1) contour plots superimposed on grey scale images of CA 5,6,7 and 8 extracted from the full AFGL 961 image. The contours shown are in ADU/sec. For CA 5 (top left) the contours base is 0.1 with a step of 0.1. For CA 6 (top right) the contour base is 0.05 with a step of 0.1. For CA 7 (bottom left) the contour base is 0.05 with a step of 0.05. For CA 8 (bottom right) the contour base is 0.1 with a step of 0.1.

removed by linear interpolation prior to ratioing. The resulting spectra of AFGL 961a, AFGL 961b and nebulosity directly south of AFGL 961b are shown in Fig. 3.

3. Results

3.1. Morphology of the region

The image of AFGL 961 shown in Fig. 1 possesses several interesting features. Present are numerous nebulous regions, some are locate relatively close to the binary while some are at a considerable distance from it. These nebulous objects are mostly

compact although in a few cases, particularly the regions directly north and east of the stars, they are extended and show distinct morphological structure. These compact nebulae are seen only in H_2; a 2.1μm narrow band continuum images of the central $2' \times 2'$ of the H_2 image shows little structure other than the stellar components in the field and some faint nebulosity in the region of AFGL 961 W. For this reason the continuum image is not presented here. The H_2/continuum images therefore confirm the spectroscopic observations in that bright pure H_2 emission nebulae possessing no significant continuum flux are present around AFGL 961. The top spectrum in Fig. 3 presents a representative region of this nebulosity located 15″ south of AFGL 961b.

The numbers in Fig. 1 identifies the nine nebulous regions found in the vicinity of AFGL 961. We herein referred to these regions as CA objects in agreement with the suggestion of the IAU Nomenclature Committee whereby NIR nebulous objects similar to morphology to optical HH objects should be designated by the first letters of the discovery authors names. Details of the CA objects in AFGL 961 are given in Table 1 where we present accurate spatial offset positions and position angles for all nine objects. Also given are morphological description of their appearance in H_2. Next, we comment on each of these objects and where possible, relate them to their optical counterparts.

CA 1 is located to the north of the binary and has the morphological appearance similar to that of an optical HH bow shock structure. This IR bow shock, shown in close-up in Fig. 4, is pure H_2 emission and is oriented with its axis of symmetry at position angle (p.a.) $\sim$354° east of north. The eastern edge of the bow shock is somewhat brighter than its western counterpart. It is uncertain which of the two stars forming the binary is the originator of this structure, although, as we shall see below (Sect. 3.2), only AFGL 961b currently shows signs of activity generally associated with outflowing gas, specifically, weak ^{12}CO bandhead emission. Tracing the axis of symmetry back from the tip of CA 1 towards the binary suggests that the identification of AFGL 961b as its originator is likely correct.

CA 2 is located to the west of the binary and is cavity- or shell-like in morphology. This source is associated with the stellar object, AFGL 961 W and briefly discussed by Hodapp (1994). AFGL 961 W is located between the two linear cavity/shell walls. A detailed view of CA 2 is shown in Fig. 4. CA 2 may be physically related to AFGL 961 W rather than the AFGL 961 binary since AFGL 961 W exhibits nebulous extensions itself (to both west and south). However, the cavity/shell walls do extend away from the approximate location of the AFGL 961 binary and there is fainter nebulous extensions joining the cavity/shell structure to the immediate vicinity of the binary itself (see Figs. 1 and 2). On the Digitized Sky Survey (SS) [2] (Fig. 7) CA 2 appears as a diffuse/nebulous regions suggesting that this is a distinct and separate PMS star unrelated to AFGL 961; being visible in the optical implies that it is either foreground to AFGL 961 (itself highly obscured in the optical) or seen through a low extinction path in the molecular cloud.

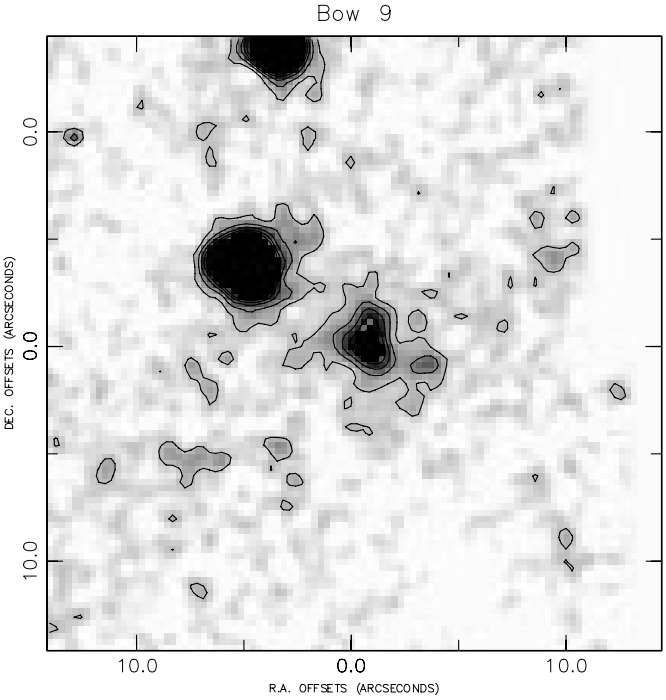

Fig. 6. S(1) contour plot superimposed on grey scale image of CA 9 extracted from the full AFGL 961 image. The contours shown are in ADU/sec and are from a base of 0.05 with a step of 0.05.

CA 3 is located to the south of the binary and, as in CA 1, exhibits a structure reminiscent of an optical bow shock. In this case however, the bow shock structure is not as definitive as in CA 1 and is confused by the close association of a second component to the west. In fact, in Fig. 2, both of these components bear much similarity to bow shock like structures. Fig. 4 shows this region in detail although the bow shock nature of these objects is not as apparent in this lower contrast image. If these two components are in fact bow shock then they are directed along axes that extend from the vicinity of the binary at p.a. $\sim$178° and $\sim$157°, respectively. The eastern bow shocks appears to lie on an axis from AFGL 961a while the western bow shock lies on an axis from AFGL 961b.

CA 4 is approximately an arcminute to the south of the binary and also has a morphology reminiscent of an optical bow shock. It can be seen more clearly in Fig. 4. The outflow axis associated with this object is $\sim$164°. This is close to halfway between the the two axes defined for CA 3 and hence, coupled with the sources physical distance from the binary, it is impossible to determine from which binary components the object originated.

CA 5 is a diffuse region of H_2 emission south-west of the binary. This object, shown in Fig. 5, possesses several distinct clumps or knots superimposed on a more diffuse nebula.

CA 6 is on the north-west edge of our image and is the most distant nebulous object detected in our images at $\sim$110″ from the binary. At the assumed distance of AFGL 961 of 1.6kpc,

[2] obtained through the SkyView facility at the NASA Goddard Space Flight Center.

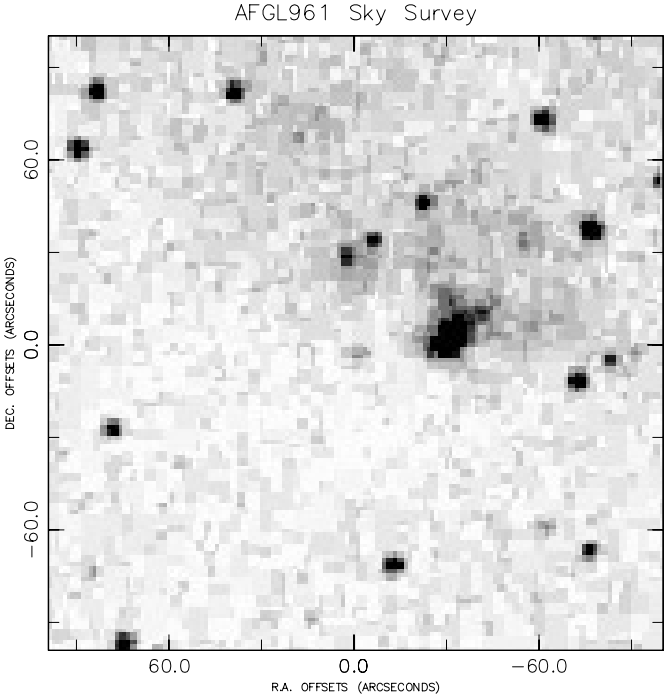

Fig. 7. Palomar Sky Survey image of the AFGL 961 region. The nebulous source AFGL 961 W is clearly visible and faintly the western of the two AFGL 961 binary components.

this corresponds to a physical separation of 0.85pc. This object, shown in Fig. 5, also consists of several bright knots with a fainter diffuse component. No identifiable morphological structure can be seen in CA 6.

CA 7 lies almost exactly halfway between the western binary component and CA 6 and along the identical axis (p.a. $\sim$36 °). CA 7 is faint but shows a definite morphological structure similar to an optical bow shock (see Fig. 1 and Fig. 5).

CA 8 also lies approximately along the axis to CA 6 and CA 7 although this object is more knotty/diffuse than CA 7, more like CA 6 in appearance (see Fig. 1 and Fig. 5). There is a hint that the fainter regions of CA 8 (see Fig. 1 a few arcseconds to the north of the peak flux) form a bow shock-like structure although deeper data is required to confirm this.

CA 9 is closer to the western edge of our image and consists of two clumps, one relatively stellar, the other diffuse with a prominent knot (see Fig. 6). Since this object was not included in the narrow band continuum image obtained, the star-like eastern component of CA 9 could possible be a field star of a young star with associated nebulosity.

3.2. NIR spectroscopy: shock-excited H_2 emission

Fig. 3 shows the 2μm spectra of both AFGL 961a, AFGL 961b and of the nebulous region located 15″ south of AFGL 961b. By far the reddest source of the binary is AFGL 961a which shows a strong rising red continuum over the wavelength regime observed. Superimposed on this is a strong Br-γ line in emission. The small-scale 'ripple' on the spectra is an artifact of the data acquisition. No other features are detected in the spectrum of AFGL 961a. Porter et al. (1998) suggested that the strong Brγ emission may be temporally variable. AFGL 961b shows a modestly rising red continuum compared to that of its companion superimposed on this spectra is also a relatively strong Br-γ emission line and also weak, but certainly identifiable, emission bands of ^{12}CO (specifically, the 2-0 ^{12}CO at 2.294μm and the 3-1 ^{12}CO at 2.323μm). The nebulosity south of AFGL 961b exhibits a spectrum of pure H_2 emission with the line emission being dominated by the v=1-0 S(1) line at 2.122μm and the Q-branch at 2.4-2.45μm. Several additional (fainter) H_2 lines are also present. No Br-γ emission is detected at this location. The spectra obtained along the long-slit used in the observations (for both binary components) show similar spectra with little to no continuum emission present.

The H_2 spectrum shown in Fig. 3 exhibits a large flux ratio (specifically 10.6) between the v=1-0 S(1) line (2.122μm) and the v=2-1 S(1) line at 2.248μm. This generally implies that the H_2 gas is shock-excited although with high enough densities (n$>10^5$ cm^{-3}) fluorescent emission (excitation by UV absorption) can produce a similar line ratio. For low density regions fluorescent excitation gives a significantly lower flux ratio (more like $\sim$2). Burton (1992) discusses the excitation of H_2 in more details. Given a number density $<10^5$, we are certainly observing shock-excited H_2 emission. The CA object corresponding to this location along the long-slit is the eastern region of CA 3 which in the deep S(1) images shown in Fig. 1 resembles a small bow shock (and would be most likely shock-excited). At the other positions along the CGS4 long-slit showing H_2 emission, the flux ratio of these two lines is similar varying only between 8 and 11. Hence, even in the presence of the high-luminosity hot binary components, the H_2 in the vicinity of the stars is probably shock-excited.

3.3. The extinction towards the H_2 emission

We can obtain an estimate of the overlying extinction towards the H_2 emission from the ratio of the two H_2 emission lines the v=1-0 Q(3) line at λ2.424 μm and the v=1-0 S(1) line at λ2.122 μm. Both these lines are emitted from the same level and their unreddened ratio has been calculated to be 0.7 (Turner et al. 1977). NIR extinction has additionally been shown to be representable by a power law of slope -1.8 (Martin & Whittet 1990). Using this we can estimate the visual extinction, A_V from the differential extinction between the two H_2 lines. At the location of the H_2 emission shown in Fig. 3, e.g. 15″ south of AFGL 961b, we find a line ratio Q(3)/S(1) of 1.16$\pm$0.2. This corresponds to a differential extinction between the two lines of 0.55$\pm$0.1 magnitudes. Extrapolating to the optical implies an overlying A_V of 29$\pm$5 magnitudes. This value is somewhat larger than the extinction derived towards AFGL 961a and AFGL 961b by Castelaz et al. (1985) e.g. $\sim$17 magnitudes. However, Alonso-Costa & Kwan (1989) and Porter et al. (1998) derived larger values of A_V, specifically, 28$\pm$4 and 20—25 magnitudes, respectively, from both NIR H line ratios (both Alonso-Costa & Kwan, and Porter et al.) and NIR contin-

uum ($\lambda < 1.5\mu$m) fitting (Porter et al.). Our value is therefore consistent with other recent determinations.

3.4. The stellar population: evidence for a PMS cluster

If one compares Fig. 1, our 2.122μm H_2 image, with the Sky Survey (SS) image shown in Fig. 7, it is obvious that the stellar population in the immediate vicinity of AFGL 961 is considerably larger in the NIR than the optical. The region centred on the AFGL 961 binary is clearly heavily obscured by overlying molecular material; few stars are found at this location in the SS image. The brightest source in the SS image is AFGL 961 W with its associated nebulosity located to the west of the centre of the image. In total, 17 stellar sources are visible in the SS image covering the region imaged in the NIR. In the H_2 image (Fig. 1) we see over 80 stellar objects. A large number of these sources are concentrated towards the centre of the image i.e. around the AFGL 961 binary. The overall impression from Fig. 1 is that there is a stellar cluster centred close to AFGL 961, in particular, on the region $\sim$30$''$ north of the binary. We confirm therefore that a small cluster, consisting of perhaps 40–50 stars, is present around the high-mass binary as originally suggested by Hodapp (1994). Further optical/NIR photometric observations in standard (broad-band) passbands are required to better investigate the cluster membership and size.

4. Discussion

4.1. Evidence for multiple outbursts

Our data implies that, within the recent history of the AFGL 961 region, there have been several phases of activity resulting in the ejection of matter which, after subsequent interaction with ambient cloud material or older ejecta from the sources, have resulted in the creation of the shock-excited H_2 emission nebulae seen in Fig. 1. The most distant H_2 feature observed (CA 6) is 0.85pc from the binary. Clearly it is a difficult task to estimate outflow velocities without quantitative information. If we assume a typical ejection velocity of $\sim$200km s^{-1}, the derived dynamical age of this feature is $\sim$4000 years. Support for this assumed ejection velocity comes from proper motion studies of HH knots (e.g. Burrows et al. 1996 for HH 30) where typical values for optical knot velocities of $\sim$200km s^{-1} have been found. Even though the energy source of HH 30 is a low-luminosity object and AFGL 961 is of considerably higher luminosity, we adopt this typical tangential velocity for the sake of our simple dynamical timescale estimates but note that our assume velocity could be in error by a factor of possibly 2–3. For CA 1, the largest and most bow-like of the H_2 features, we obtain a dynamical age of 1200 years. For CA 3, the bow shock structure lying to the south of the binary, a dynamical age of 800 years is found. These simple timescale estimates, coupled with the multiple outflow axes found, suggests that multiple outburst events have obviously occurred in AFGL 961 over a period of at least the last 4000 years. Performing the same calculation for all observed H_2 nebulae suggests a typical inter-outburst timescale of between 500 and 750 years. In optical HH objects, a typical timescale for the formation of working surfaces/bow shocks is thought to be $\sim$500 years between events. In low-mass PMS objects such as T Tauri stars, these outbursts are being linked to disk accretion events resulting in outbursts of the FU Orionis (FUor) type (Reipurth & Aspin, 1997). AFGL 961 is considerably more luminous than either the typical energy source of an optical HH object or a typical FUor, specifically, $L_{AFGL\ 961}$ $\sim$7500$L_\odot$ whereas a typical HH energy source (HHES) has L_{HHES} <1000$L_\odot$and can be as low as a few $L_\odot$ (e.g. $L_{HH\ 43IRS}$ $\sim$5$L_\odot$). One exception to this is the exciting source of the large-scale HH flow HH 80/81 (Reipurth & Graham, 1988) namely GGD 27 (Aspin et al. 1991) which has L_{bol} $\sim$6000$L_\odot$. The most luminous FUor found to date is Z CMa (the energy source of a HH 160) which has L_{bol} $\sim$600$L_\odot$. It seems however, that the inter-outburst timescales for all these classes of objects are perhaps related and not obviously dependent on source luminosity.

Clearly our assumed ejection velocity of 200km s^{-1} critically effects the derived outburst timescales. Also, the relation between physical ejection velocity (of gas) and shock velocity (producing H_2 emission) is not a trivial matter since it is related to the velocity difference between the outflowing material and that of the material upon which it impacts. In the case of impact on previous ejecta from the originating source, the shock velocity can be lower than the ejection velocity. H_2 dissociation would occur in regions with shock velocities >50km s^{-1} so for planar shocks 200km s^{-1} is a clearly impractical. However, often found in reality are oblique shocks whereby the shock direction is not orthogonal to the 'outflow' direction. In these cases only the orthogonal component of the shock velocity need be considered. This would clearly lower the effective shock velocity. Clearly, a through observational study of the velocity structure of both the outflowing gas and the gas upon which it is impacting is required before further conclusive comparative work be undertaken. What we can state here is that eruptive events similar in timescale to those occurring in FUors involving variable accretion rates, the buildup of disk material and eventual mass-dumping from disk to photosphere resulting in a significant luminosity increase and ejection of matter/shocks manifesting as HH objects and jets (and in embedded sources, NIR shock-excited structures), are consistent with what we have found observationally in AFGL 961.

4.2. Evidence for non-axially symmetric outflow axes

What is also obvious from the structure seen in our images is that the repetitive ejection of matter resulting in the shock-excited H_2 emission observed has clearly occurred along more than a single axis originating at the binary components i.e. the activity has been non-axially symmetric over time. One axis can be traced north-south from CA 1 through AFGL 961b to CA 3. Another axis is clearly defined from CA 6 through CA 7, through the binary system and onto CA 5. Other single feature axes are also defined from the binary towards both CA 4, and CA 8. Both of these outburst axes have no detectable counterparts on the opposite side of the binary. It is unclear whether the H_2 seen closeby

AFGL 961 W is associated with AFGL 961 or whether it is resultant from activity in AFGL 961 W itself, however, from the clearly defined axes present around AFGL 961 we can trace four distinct directions along which activity has been directed. At the present time, only AFGL 961b shows direct observational evidence for activity (in the form of the weak CO bandhead emission at 2.294 μm) which when viewed in combination with the thermal infrared excess exhibited (Castelaz et al. 1985) and the fact that the extinction towards the source is relatively low (A_V=16.7 magnitudes (Castelaz et al. 1985) indicates the presence of a dense, hot, inclined accretion disk. AFGL 961a was found to be coincident with a compact HII region (0.59″ Bally & Predmore 1983) suggesting that it also has significant (ionized) circumstellar material possibly also in the form of an accretion disk. AFGL 961a clearly possess a strong thermal excess (see Fig. 3) and has a line-of-sight extinction similar to that of AFGL 961b (i.e. A_V=17 magnitudes; Castelaz et al. 1985). It is not possible to determine the precise origin of the outflow axes within the binary since the H_2 features seen are relatively diffuse with no associated jet-like structures as often seen in the optical. Since multiple outflow axes are present, it would seem feasible to assume that at one time both AFGL 961a and AFGL 961b have contributed to the shock-excited emission observed. One possible scenario for the multiple outflow axes is that binary orbital motion coupled with accretion disk axial precession have caused significant deviations of the polar (outflow) axes of the stars with time. Alternatively, if both stars have produced outflow activity in the past then their respective polar/outflow axes are not aligned and not orthogonal to the binary orbital plane.

5. Further observational requirements

Clearly additional observations of AFGL 961 and its associated NIR shock-excited nebulosities are required to better understand its structure and evolution. Deeper H_2 images over a wider field may reveal additional (and possibly more distant) H_2 features. Deep broad-band NIR observations will determine the extent of the PMS cluster around the source and allow the investigation of the age and mass/luminosity function of the region. Higher resolution NIR spectroscopy of the H_2 would give more quantitative information on the shock velocities and geometry of the outflowing material while high resolution mm/sub-mm CO line observations would aid in the study of the ejection velocity and velocity structure of the ambient medium or earlier ejecta upon which the outflows are impacting. High resolution sub-mm continuum observations may also shed light on the evolutionary state of the two binary components.

Acknowledgements. We thank the staff at UKIRT for their support during the acquisition of the data presented above. Some additional data was obtained through the SkyView facility at the NASA Goddard Space Flight Center. We also thank Bo Reipurth for reading the manuscript before submission and making several valuable suggestions for improvement.

References

Alonso-Costa, J.L., Kwan, J.: 1989, ApJ, 338, 403
Aspin, C., Casali, M.M., Geballe, T.R., McCaughrean, M.J., 1991, A&A, 252, 299
Aspin, C., Sandell, G., Russell, A.P.G., 1994, A&AS, 106, 165
Bally, J., Predmore, R., 1983, ApJ, 265, 778
Böhm, K.-H., Perry, J.F., Schwartz, R.D., 1973, ApJ, 179, 149.
Burrows, C.J., et al., 1996, ApJ, 473, 437
Burton, M.G., 1992, Aust. J. Phys., 45, 463
Castelaz, M.W., Grasdalen, G.L., Hackwell, J.A., Capps, R.W., Thompson, D., 1985, AJ, 90, 1113
Davis, C.J., Dent, W.R.F., Matthews, H.E., Aspin, C., Lightfoot, J.F., 1994a, MNRAS, 26, 933
Davis, C.J., Eislöffel, J., Ray, T.P., 1994b, ApJ, 426, 93
Dopita, M.A., Evans I., Schwartz, R.D., 1982, ApJLet, 263, L73
Eislöffel, J., Davis, C.J., Ray, T.P., Mundt, R., 1994, ApJ, 422, 91
Eislöffel, J, 1997, Proc. of IAU Symp. 182 on 'Herbig-Haro Flows and the Birth of Low Mass Stars', 20-24 January 1997, Chamonix, France, eds. B. Reipurth and C. Bertout, p93.
Grasdalen, G.L., Gehrz, R.D., Hackwell, J.A., Castelaz, M., Gullixson, C., 1983, ApJS, 53, 413
Herbig, G.H., 1951, ApJ, 113, 697
Hodapp, K.-W., 1994, ApJS, 94, 615
Hodapp, K.-W., Ladd, E.F. 1995, ApJ, 453, 715
Lada, C.J., Gautier III, T.N., 1982, ApJ, 261, 161
Lenzen, R., Hodapp, K.W., Reddmann, T., 1984, A&A, 137, 365
Martin, P.G., Whittet, D.C.B., 1990, ApJ, 357, 113
McCaughrean, M.J., Rayner, J.T., Zinnecker, H., 1994, ApJ, 436, 189
Mountain, C.M., Robertson, D., Lee, T.J., Wade, R., 1990, SPIE v1235 p25
Porter, J.M., Drew, J.E., Lumsden, S.L.: 1998, A&A, preprint.
Puxley, P.J., Sylvester, J., Pickup, D. et al., 1994, SPIE, v2198, p350
Reipurth, B., Aspin C., 1997, AJ, AJ, 114, 2700
Reipurth, B. 1989, Nat, 340, 42
Reipurth, B., Graham, J.A., 1988, A&A, 202, 219
Reipurth, B., Heathcote, S., 1992, A&A, 257, 693
Sandell, G., Aspin, C.: 1998, A&A, in preparation.
Turner, D.G., 1976, ApJ, 210, 65
Turner, J., Kirby-Docken, K., Dalgarno, A., 1977, ApJS, 35, 281